

Plasma simulation to analyze velocity distribution characteristics of pseudospark-sourced electron beam

Hai-Long Li(李海龙), Chen-Fei Hu(胡陈飞), Che Xu(徐彻), Yong Yin(殷勇), Bin Wang(王彬), Lin Meng(蒙林), Mao-Yan Wang(王茂琰)

Citation: Chin. Phys. B . 2020, 29(10): 105101 . **doi:** 10.1088/1674-1056/aba274
Journal homepage: http://cpb.iphy.ac.cn; http://iopscience.iop.org/cpb

What follows is a list of articles you may be interested in

Effect of aperture field distribution on the maximum radiated power at atmospheric pressure

Pengcheng Zhao(赵朋程), Lixin Guo(郭立新)

Chin. Phys. B . 2017, 26(11): 115101 . **doi:** 10.1088/1674-1056/26/11/115101

Effect of electrical discharge in water on concentration of nitrate solution

F Sohbatzadeh, H Bagheri, R Safari

Chin. Phys. B . 2017, 26(2): 025101 . **doi:** 10.1088/1674-1056/26/2/025101

Initiation of vacuum breakdown and failure mechanism of the carbon nanotube during thermal field emission

Dan Cai(蔡丹), Lie Liu(刘列), Jin-Chuan Ju(巨金川), Xue-Long Zhao(赵雪龙), Hong-Yu Zhou(周泓宇), Xiao Wang(王潇)

Chin. Phys. B . 2016, 25(4): 045101 . **doi:** 10.1088/1674-1056/25/4/045101

Effect of microwave frequency on plasma formation in air breakdown at atmospheric pressure

Zhao Peng-Cheng, Guo Li-Xin, Li Hui-Min

Chin. Phys. B . 2015, 24(10): 105102 . **doi:** 10.1088/1674-1056/24/10/105102

Experimental investigation of effects of airflows on plasma-assisted combustion actuator characteristics

Liu Xing-Jian, He Li-Ming, Yu Jin-Lu, Zhang Hua-Lei

Chin. Phys. B . 2015, 24(4): 045101 . **doi:** 10.1088/1674-1056/24/4/045101

Plasma simulation to analyze velocity distribution characteristics of pseudospark-sourced electron beam*

Hai-Long Li(李海龙)[1,†], Chen-Fei Hu(胡陈飞)[1], Che Xu(徐彻)[1], Yong Yin(殷勇)[1], Bin Wang(王彬)[1], Lin Meng(蒙林)[1], and Mao-Yan Wang(王茂琰)[2]

[1] *School of Electronic Science and Engineering, University of Electronic Science and Technology of China, Chengdu* 610054, *China*
[2] *School of Physics, University of Electronic Science and Technology of China, Chengdu* 610054, *China*

(Received 25 February 2020; revised manuscript received 26 June 2020; accepted manuscript online 3 July 2020)

Pseudospark-sourced electron beam is a promising candidate for driving vacuum electronic devices to generate millimeter wave and terahertz wave radiation as it has a very high combined beam current density. However, the inherent velocity spread of the beam, which is difficult to measure in experiment, has a great influence on the operating frequency and efficiency of the vacuum electronic device. In this paper, the velocity distribution characteristics of the electron beam produced by a single-gap hollow cathode electron gun are numerically studied and a three-dimensional kinetic plasma simulation model of a single-gap hollow cathode electron gun is built by using particle in cell and Monte Carlo collision methods in Vorpal. Based on the simulation model, the time-dependent evolution of the plasma formation inside the hollow cathode and electron beam generation process are observed. It is demonstrated that the pseudospark-sourced electron beam has a relatively large velocity spread. The time-dependent velocity distribution of the beam is analyzed, and the dependence of the beam velocity distribution under various operating conditions such as anode–cathode potential difference, gas pressure, and cathode aperture size are also studied.

Keywords: pseudospark, hollow cathode, vacuum electronic devices, discharge

PACS: 51.50.+v , 29.25.–t, 29.25.Bx **DOI:** 10.1088/1674-1056/aba274

1. Introduction

The pseudospark (PS) discharge phenomenon was discovered in 1970s and shortly after that it was developed as an electron beam source first by Christiansen and Schultheiss.[1] The typical PS discharge device consists of two plane-parallel electrodes with an axial bore hole and a hollow region behind each of them, often called hollow cathode (HC). The HC can provide high intensity pulsed electron beam with a fast current rising rate when operating on the left-hand side (with respect to the minimum) of the HC analogy to the Paschen's curve.[2] It can be operated with various gases (*e.g.*, nitrogen, argon, hydrogen, xenon, *etc.*) and different electrode materials (*e.g.*, tungsten, copper, steel, *etc.*). These characteristics made the HC suitable for a variety of applications.[3–7]

To date, the vacuum electronic devices (VEDs) is still a main method to achieve millimeter wave radiation of high power. However, this kind of device usually requiires high quality intense electron beams. The current density of a PS-sourced electron beam could reach up to 10^4 A/cm^2 or-more and it had the ability to self-focus because of the ion channel.[8] It was demonstrated that the electron beam pulses with a 3-mm diameter could be transported up to 20 cm without a guiding magnetic field.[9] Therefore, the use of PS-source electron beam to enable VEDs to achieve millimeter wave and terahertz wave radiation is a promising method. Some researchers have achieved hundreds of watts output power at W-band through the extended interaction oscillators based on PS-sourced electron beam,[10–12] similarly a 0.2-THz backward wave oscillator based on PS-sourced electron beam with a maximum power of 20 W has also been realized in recent years.[6]

There are many experimental studies on PS-sourced plasma cathode electron gun (also called HC electron gun), and what are easily measured in experiment were only discharge voltage, discharge current and electron beam current.[13–16] Numerical simulation was also a feasible method with the help of particle in cell (PIC) and Monte Carlo collision (MCC) methods.[17–22] Some researchers studied the discharge mechanism by simulating the PS discharge,[17–20] and others investigated the influences of various operating conditions on the discharge current.[20–22] However, the electron beam produced by the PS-sourced may have a relatively large velocity spread due to the collisions of electrons with other particles. It was demonstrated that the inherent velocity spread of the PS-sourced electron beam had a great influence on the operating frequency and efficiency of the VED.[23] But the beam velocity distribution is difficult to measure in experiment and simulation researches are lacking. Therefore, research on the velocity distribution characteristics of the PS-

*Project supported by the Sichuan Science and Technology Program, China (Grant No. 2019YJ0188) and the National Natural Science Foundation of China (Grant Nos. 61671116 and 11905026).

†Corresponding author. E-mail: hailong703@163.com

© 2020 Chinese Physical Society and IOP Publishing Ltd

sourced electron beam is of great significance. In this paper, an investigation of single-gap HC electron gun is carried out by three-dimensional (3D) kinetic plasma simulation in Vorpal 4.2 version.[24] The investigation covers the time-dependent velocity distribution characteristics of the PS-sourced electron beam, and its dependence on operation conditions such as anode–cathode potential difference, gas pressure, and cathode aperture size.

In this paper, we build a 3D kinetic plasma simulation model of a single-gap hollow cathode electron gun with PIC and MCC methods in Vorpal, since 3D simulation was closer to the real physical model than two-dimensional (2D) simulation. UIsing this model, we study the time-dependent properties of PS-sourced electron beam and then analyze the velocity distribution of the PS-sourced electron beam under various operating conditions. Finally, we draw some conclusions form the present study.

2. Model description

The 2D schematic view of a simulated structure used for the single-gap HC electron gun is illustrated in Fig. 1. During simulation, all electrodes are made of copper, the whole area is filled with argon gas at a certain pressure and at room temperature, and a negative high voltage is applied to the cathode (both anode and collector are set to be zero potential). When it works, the discharge occurs in the cathode cavity, the electrons are absorbed at anode and collector. As shown in Fig. 1, the specific sizes are as follows: $L_1 = L_2 = 50$ mm, $L_3 = 3$ mm, $L_4 = 0.5$ mm, $W_1 = W_2 = 1$ mm, $D_1 = D_2 = 3$ mm, gas pressure varies from 10 Pa to 40 Pa, and the cathode voltage varies from -6 kV to -14 kV.

In order to simulate the evolution of plasma more realistically, the physical processes considered in the simulation are shown in Table 1.

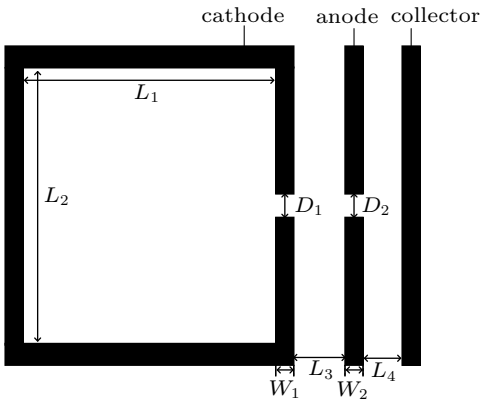


Fig. 1. 2D schematic view of simulated structure.

Table 1. Physical processes in simulation.

Collision	elastic collisions between electrons and argon atoms
	excitation collisions between electrons and argon atoms
	ionization collisions between electrons and argon atoms
Boundary	electrons and argon ions absorbed by metal boundary
	secondary electrons from argon ions impacting on the metal surfaces

The PIC parameters count in plasma simulation such as cell size, time step, and particle weighting (the actual number of particles represented by a macro particle) are set to be 0.25 mm, 10^{-12} s, and 4×10^6 respectively. The same quantities of seed electrons and seed ions with 2.5-eV random thermal energy are randomly distributed in the cathode cavity, because a certain number of electrons are necessary to initiate the discharge.[25]

3. Results and analyses

Using the simulation model discussed in the previous section, a series of computer simulations is carried out. Under the conditions of cathode voltage of -10 kV and gas pressure of 30 Pa, the required seed electrons and ions are loaded into the cathode cavity. Initially, due to the special geometry of the electron gun, the anode–cathode potential difference forms an axisymmetric electric field directed from the cathode aperture to the inner wall of the cathode cavity. Under the electric field driving, since the ion mass is much larger than the electron mass, the ions are almost stationary and the electrons move quickly inside the cathode cavity until they are emitted from the cathode cavity and fall to the anode.[20] The probability of collision ionization between the electrons and neutral gas particles greatly increases because of electrons' movement. Therefore, denser plasmas are generated inside the cathode.

The electrons emitted from the cathode cavity make the number of ions greater than the number of electrons, which results in the virtual anode growing near the cathode aperture inside the cathode cavity from the viewpoint of the potential distribution.[13] The potential distribution and electrons' distribution at 11 ns are shown in Figs. 2(a) and 2(b), respectively, wherein about -7.5 kV potential starts to penetrate the inside of the cathode cavity, and lots of new electrons are generated near the cathode aperture through the collision ionization and secondary electrons. The virtual anode causes a stronger electric field inside the cathode cavity, which in turn leads to the fact that the electrons are attracted toward the cathode aper-

ture. The collision ionization and the formation of the virtual anode promote each other continuously, and then an intense discharge occurs. Eventually, all the electrons are confined to the virtual anode region, and the kinetic energy of the electrons begins to decrease because of the relatively weak electric field in the virtual anode region and the collisions. So the collision ionization begins to decrease and discharge current decreases as well. At 15 ns (peak discharge current moment), figure 2(c) shows that about −4 kV virtual anode is generated inside the cathode cavity, and figure 2(d) shows that almost all the electrons are confined to the virtual anode region. Apparently, the potential change in the virtual anode region is relatively small.

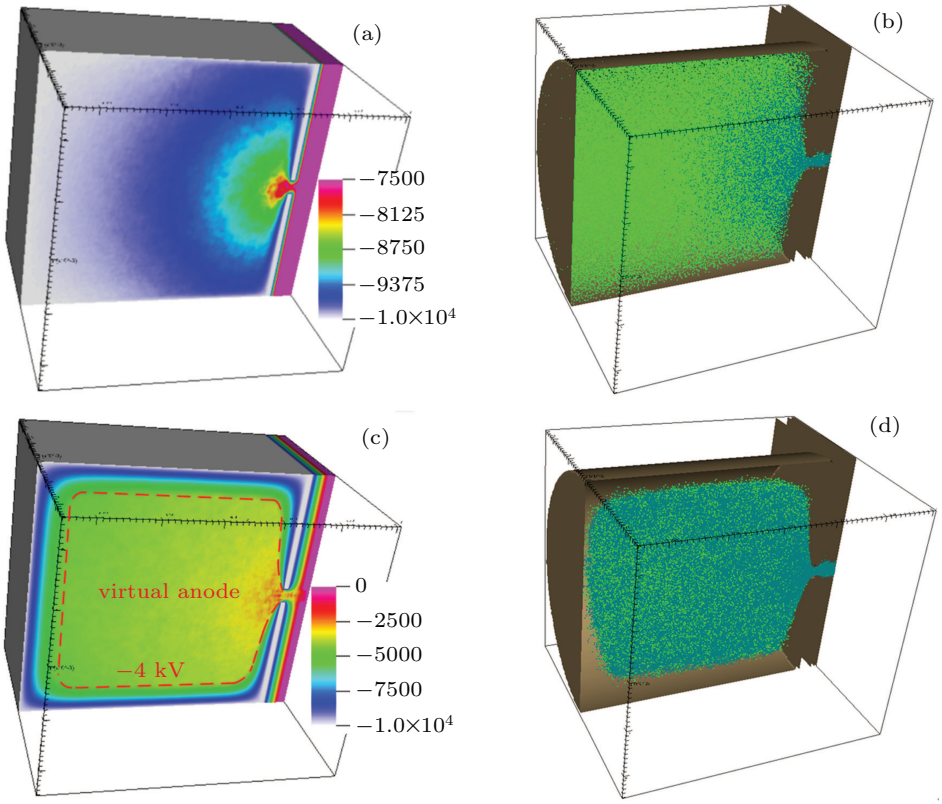


Fig. 2. At cathode voltage −10 kV and gas pressure 30 Pa: (a) potential distribution at 11 ns, (b) seed electrons (green) and new electrons (blue) distribution at 11 ns, (c) potential distribution at 15 ns, and (d) seed electrons (green) and new electrons (blue) distribution at 15 ns.

According to the simulation results, it can be found that the discharge process in the simulation is in accordance with the conclusions of other researchers,[17,19,22] which proves the effectiveness of the simulation.

3.1. Time-dependent properties of PS-sourced electron beam

Firstly, the simulation results of the HC electron gun under the conditions of cathode voltage of −10 kV and gas pressure of 30 Pa are taken as a representative example, and the data of the electrons absorbed by the collector are analyzed. Figure 3(a) shows the waveform of discharge current and the beam current, with the discharge period of about 10 ns and the peak discharge current appears at 15.1 ns.

With the discharge proceeding, the collision ionization and the formation of virtual anode promote each other. The electrons produced by collision ionization at different moments and different locations have different initial potential energy. As a result of the collision, their directions of motion are changed and kinetic energy is lost until they leave the cathode cavity. As the virtual anode penetrates the cathode cavity, the initial potential energy of the newly generated electrons decreases, and the kinetic energy of the previously generated electrons decreases due to collisions, so the mean kinetic energy of the emitted electrons decreases gradually, and their axial mean velocity decreases with time as well,which is shown in Fig. 3(b). Before 8 ns, the electron beam velocity is not counted as the beam current is too small (less than 1 A).

During the discharge, the electrons generated at different moments accumulate in the cathode cavity. For electrons, the difference in kinetic energy becomes larger and larger because of different initial potential energy values and different times of collisions, thus the velocity spread of the electron beam appears to increase with time going by. The beam velocity distributions at three different moments are shown in Fig. 3(d) (the velocity interval 0 m/s–7×10^7 m/s is considered as a unit length, and the integral of velocity distribution density is taken as unity in this interval, the following velocity distribution figures are all represented in this way), it can be found that the

PS-sourced electron beam does have a relatively large velocity spread at any moment and the beam velocity distributions at different moments differ from each other greatly. Moreover, the mean kinetic energy of the electrons at peak discharge current moment is about 25% of the initial potential energy of the seed electrons.

The movement of electrons is mainly in the radial direction because of the potential distributions shown in Figs. 2(a) and 2(c). The kinetic energy of the electrons increases with the formation of virtual anode but decreases with all electrons confined to the virtual anode, so the mean radial velocity of electron beam first increases and then decreases with time, which is shown in Fig. 3(c).

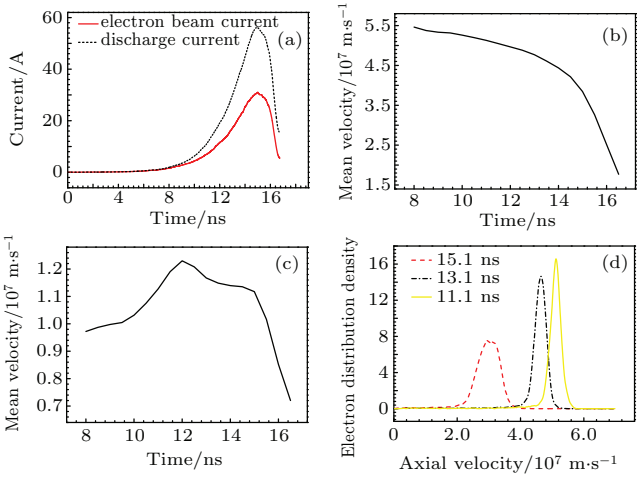


Fig. 3. Time-dependent properties of PS-sourced electron beam, showing (a) waveform of discharge current and beam current, (b) time-dependent axial mean velocity of electrons, (c) time-dependent radial mean velocity of electrons, and (d) electron beam velocity distributions at different moments.

4. Comparison among velocity distributions of PS-sourced electron beam under various operating conditions.

The beam current and its velocity distribution are the main performance indexes of the electron gun. Generally, the operating condition of an electron gun has an important influence on these characteristics. The beam velocity distributions at different moments can hardly be measured for the HC electron gun, so the simulation research on this problem is of great significance. Based on the simulation model mentioned in the second section, the effects of gas pressure, cathode aperture size and cathode voltage on beam velocity distribution can be studied by setting various operating conditions. However, the discharge duration and beam current are different under various operating conditions, so the axial velocity distribution of the electron beam at the peak current moment is taken as the contrast.

The simulation results indicate that the beam current of the HC electron gun increases with the increase of the gas pressure.[20] In order to study the influence of gas pressure on the beam velocity distribution, the cathode voltage is set to be −10 kV. Then the simulation data from different gas pressures are analyzed and the axial velocity distributions of the electron beams at peak current moment are shown in Fig. 4(a), it is obvious that the axial mean velocity of electrons decreases with the increase of gas pressure. Because the mean free path of electrons decreases proportionally with gas pressure increasing, the increase in gas pressure leads the number of electron collisions to increase and consequently the electrons lose more kinetic energy. Moreover, it can be seen from Fig. 4(a) that the greater the gas pressure, the greater the beam velocity spread is.

The anode–cathode potential difference will affect the potential distribution, which in turn affects the initial potential energy of electrons, so it may have a great influence on the beam velocity distribution. When the gas pressure is 30 Pa, figure 4(b) shows the axial velocity distribution of the electron beam under different cathode voltages. It can be found that the larger the potential difference, the larger the axial mean velocity of the electron beam is, since the initial potential energy of the electrons increases with anode–cathode potential difference increasing. At the same time, the velocity spread difference of the electron beam is very small under different potential differences, so the electron beam with higher kinetic energy can be achieved by increasing the anode–cathode potential difference.

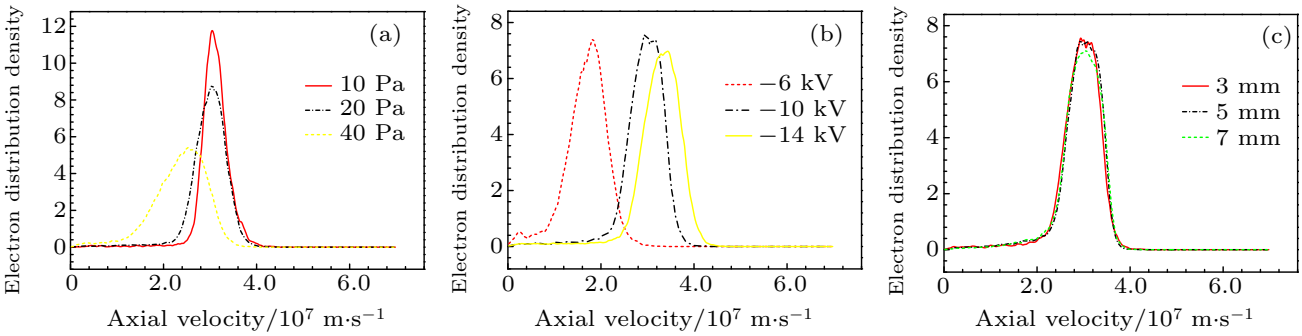


Fig. 4. Axial velocity-dependent electron density distributions of electron beam at (a) different gas pressures, (b) different cathode voltages, and (c) different cathode aperture sizes.

The larger the cathode aperture, the larger the diameter of the electron beam is. The beam current is also a function of cathode aperture size.[19,20] The larger the cathode aperture, the easier the virtual anode in the cathode cavity forms, and the more likely the electrons emit from the cathode cavity. However, the simulation results show that the difference in cathode aperture size has little effect on the axial velocity distribution of the electron beam. When the gas pressure is 30 Pa and the cathode voltage is −10 kV, the axial velocity distributions of the electron beams with different cathode aperture sizes are shown in Fig. 4(c). Clearly the axial velocity distributions of the electron beams obtained from the cathode aperture sizes ranging from 3 mm to 7 mm are only slightly different.

5. Conclusions

In this paper, using PIC and MCC methods in Vorpal, a 3D model of a single-gap HC electron gun is established. The velocity distribution characteristics of the PS-sourced electron beam at different moments during the discharge are obtained by plasma simulation under various operating conditions. With the discharge proceeding, the beam velocity distributions at different moments are quite different, the axial velocity of the electron beam shows accelerating declines while the velocity spread increases obviously, and the electron beam produced by the PS-sourced has a relatively large velocity spread at any moment. Moreover, the radial velocity first increases and then decreases. Therefore, only the electron beam with a certain time period is required by the VEDs, because only the electron beam in a certain velocity range can drive the VEDs.

The influence of operation condition on the velocity distribution of the PS-sourced electron beam is studied. The simulation results clearly indicate the effects of anode–cathode potential difference, gas pressure and cathode aperture size. When other configurations are fixed, the simulation results show that the higher the anode–cathode potential difference, the larger the axial mean velocity of the electron beam is, but there is little difference in velocity spread. As the gas pressure increases, the axial mean velocity of the electron beam decreases while the axial velocity spread increases significantly. In addition, the change in cathode aperture size has little effect on the axial velocity distribution. However, the beam velocity distribution still cannot be predicted according to the cathode–anode potential difference and gas pressure, but the kinetic energy of the electron beam can increase and the velocity spread can decrease by increasing the cathode–anode potential difference and reducing the gas pressure. This investigation will undoubtedly provide a more in-depth understanding of the characteristics of PS-sourced electron beam, and thus conducing to its applications.

Acknowledgement

We thank Southwestern Institute of Physics very much for helping us run the Vorpal code.

References

[1] Christiansen J and Schultheiss C 1979 *Z. Physik A* **290** 35
[2] Cross W, Yin H, He W, Ronald K, Phelps A D R and Pitchford L C 2007 *J. Phys. D: Appl. Phys.* **40** 1953
[3] Frank K, Boggasch E, Christiansen J and Goertler A 1988 *IEEE T. Plasma Sci.* **16** 317
[4] Akhmadeev Yu H, Denisov V V, Koval N N, Kovalsky S S, Lopatin I V, Schanin P M and Yakovlev V V 2017 *Plasma Phys. Rep+.* **43** 67
[5] Tkotz R, Gortler A, Christiansen J and Dollinger S 1995 *IEEE T. Plasma Sci.* **23** 309
[6] He W, Zhang L, Bowes D, Yin H, Ronald K, Phelps A D R and Cross A W 2015 *Appl. Phys. Lett.* **107** 133501
[7] Korolev Y D and Koval N N 2018 *J. Phys. D: Appl. Phys.* **51** 323001
[8] Bowes D, Yin H, He W, Ronald K, Phelps A D R, Chen D, Zhang P, Chen X, Li D and Cross A W 2014 *IEEE T. Plasma Sci.* **42** 2826
[9] Yin H, Cross A W, He W, Phelps A D R, Ronald K, Bowes D and Robertson C W 2009 *Phys. Plasmas* **16** 063105
[10] Zhao J, Yin H, Zhang L, He W, Zhang Q, Phelps A D R and Cross A W 2017 *Phys. Plasmas* **24** 060703
[11] Yin Y, He W, Zhang L, Yin H, Robertson C W and Cross A. W 2016 *IEEE T. Electron Dev.* **63** 512
[12] Shu G X, Yin H, Zhang L, Zhao J P, Liu G, Phelps A D R. Cross A W and He W 2018 *IEEE Electron Dev. Lett* **39** 432
[13] Stetter M, Felsner P, Christiansen J, Gortler A, Hintz G, Mehr T, Stark K and Tkotz R 1995 *IEEE T. Plasma Sci.* **23** 283
[14] Arsov V and Frank K 2007 *IEEE T. Plasma Sci.* **35** 83
[15] Hu J, Rovey J L and Zhao W 2017 *Rev. Sci. Instrum.* **88** 013302
[16] Zhang J and Liu X 2017 *Plasma Chem. Plasma P.* **37** 1211
[17] Gu X W, Meng L, Yan Y and Sun Y Q 2009 *J. Infrared Millim. TE.* **30** 1083
[18] Varun, Dwivedi H K and Pal U N. 2018 *IEEE T. Electron Dev.* **65** 4607
[19] Zhang J, Liu X and Zhang Q 2017 *Phys. Plasmas* **24** 053515
[20] Varun and Pal U N 2018 *IEEE T. Electron Dev.* **65** 1542
[21] Cetiner S O, Stoltz P, Messmer P and Cambier J L 2008 *J. Appl. Phys.* **103** 023304
[22] Pal U N, Prajapati J, Kumar N and Prakash R 2015 *Indian J. Phys.* **89** 951
[23] Zhang Z, Yin Y, Bi L J, Chang Z W, Xu C P, Wang B and Meng L 2017 *Phys. Plasmas* **24** 043103
[24] Nieter C and Cary J R 2004 *J. Comput. Phys.* **196** 448
[25] Mehr T, Arenz H, Bickel P, Christiansen J, Frank K, Gortler A, Heine F, Hofmann D, Kowalewicz R and Schlaug M 1995 *IEEE T. Plasma Sci.* **23** 324